Electronic Supplementary Information

Volatilizable and Cost-effective Quinone-Based Solid Additives for Improving Photovoltaic Performance and Morphological Stability in Non-Fullerene Polymer Solar Cells

Youdi Zhang,[‡,ab] Yongjoon Cho,[‡,a] Jungho Lee,[a] Jiyeon Oh,[a] So-Huei Kang,[a] Sang Myeon Lee,[a] Byongkyu Lee,[a] Lian Zhong,[a] Bin Huang,[a] Seungjin Lee,[c] Jin-Woo Lee,[c] Bumjoon J. Kim,[c] Yongfang Li[d] and Changduk Yang*[,a]

[a] *Department of Energy Engineering, School of Energy and Chemical Engineering, Perovtronics Research Center, Low Dimensional Carbon Materials Center, Ulsan National Institute of Science and Technology (UNIST), 50 UNIST-gil, Ulju-gun, Ulsan 44919, Republic of Korea*

Email: yang@unist.ac.kr

[b] *College of Chemistry, Nanchang University, 999 Xuefu Avenue, Nanchang 330031, China*

[c] *Chemical and Biomolecular Engineering, Korea Advanced Institute of Science and Technology (KAIST), Daejeon, 34141, Republic of Korea*

[d] *Beijing National Laboratory for Molecular Sciences, CAS Key Laboratory of Organic Solids, Institute of Chemistry, Chinese Academy of Sciences, Beijing 100190, China*

[‡]Y. Zhang and Y. Cho contributed equally to this work.

Solar cell fabrication and characterization

The PSCs were fabricated with a configuration of ITO/PEDOT:PSS/active layer/PDINO/Al, where ITO, PEDOT:PSS, and PDINO refer to indium tin oxide, poly(3,4-ethylenedioxythiophene):poly(styrene sulfonate), and perylene diimide functionalized with amino N-oxide, respectively. PEDOT:PSS (Bayer Baytron 4083) was spin coated at 4000 rpm onto the ITO substrate, followed by annealing at 150 °C for 15 min in air. The active layer was spin coated from chloroform solutions, followed by a thermal annealing treatment at 140 °C for 10 min. The total concentration of blend solution was 16 mg mL^{-1}, and the donor:TPT10 ratio was kept at 1:1.2. SA-x of the same concentration was also dissolved in chloroform. Then methanol solution of PDINO (1.0 mg mL−1) was then deposited onto the active layer with a spin rate of 3000 rpm for 30 s. Finally, 100 nm aluminum was thermally evaporated under vacuum ($< 3.0 \times 10^{-6}$ Pa). The active area of each sample was 13.0 mm^2. The current density versus voltage (*J*–*V*) characteristics were recorded using a Keithley 2400 source under illumination of an AM 1.5G solar simulator with an intensity of 100 mW cm^{-2}. The EQE measurements were conducted using Model QEX7 by PV measurements Inc. (Boulder, Colorado) in ambient air. The thickness of the active layers was measured using a stylus profilometer (P6, KLA Tencor).

SCLC measurements

The hole and electron mobilities were measured via using the space charge limited current (SCLC) method. Device structures are ITO/PEDOT:PSS/active layer/Au for hole-only devices and ITO/ZnO/active layer/PDINO/Al for electron-only devices,

respectively. The SCLC mobilities were calculated using the Mott–Gurney equation, $J = 9\varepsilon_r\varepsilon_0\mu V_2/8L_3$, where εr is the relative dielectric constant of the organic semiconductor, ε_0 is the permittivity of empty space, m is the mobility of zero-field, L is the thickness of the active layer, and $V = V_{applied} - V_{built\text{-}in} - V_{series\text{-}resistance}$ (the V_{bi} values are 0.2 and 0 V for the hole-only and the electron-only devices, respectively), where $V_{applied}$ is the voltage applied and $V_{built\text{-}in}$ is the built-in voltage from the relative work function difference between the two electrodes. $V_{series\text{-}resistance}$ is the voltage caused by the series and contact resistance potential drop ($V_{series\text{-}resistance} = J \times R_{series\text{-}resistance}$). For convenience, the voltage drops caused by this resistance ($R_{series\text{-}resistance}$) was ignored.

Atomic force microscopy (AFM)

The atomic force spectroscopy (AFM) images of blend films were recorded using the Agilent 5500 scanning probe microscope running with a Nano scope V controller.

GIWAXS characterization

The GIWAXS measurement was carried out at PLS-II 6A U-SAXS beamline of the Pohang Accelerator Laboratory in Korea. The X-rays coming from the in-vacuum undulator (IVU) were monochromated (wavelength λ = 1.10994 Å) using a double crystal monochromator and focused both horizontally and vertically (450 (H) × 60 (V) μm^2 in FWHM @ sample position) using K-B type mirrors. The GIWAXS sample stage was equipped with a 7-axis motorized stage for the fine alignment of the sample, and the incidence angle of X-ray beam was set to be 0.11º ~ 0.13º for the neat and blend films. GIWAXS patterns were recorded with a 2D CCD detector (Rayonix SX165) and X-ray irradiation time within 100 s, dependent on the saturation level of the detector.

Diffraction angles were calibrated using a sucrose standard and the sample-to-detector distance was ~231 mm.

R-SoXS characterization

R-SoXS transmission measurements were performed with the photon energy of 284.2 eV at beamline 11.0.1.2 at the Advanced Light Source. Samples for R-SoXS measurement were prepared on a PSS modified Si substrate under the same conditions as those used for device fabrication and then transferred by floating in water to a 1.5 × 1.5mm, 100 nmthick Si_3N_4 membrane supported by a 5 × 5 mm, 200 mm thick Si frame (Norcada Inc.). 2D scattering patterns were collected on an in-vacuum charge-coupled device (CCD) camera (Princeton Instrument PI-MTE). The sample detector distance was calibrated from diffraction peaks of a triblock copolymer poly (isoprene-b-styrene-b-2-vinyl pyridine), which has a known spacing of 391 A°. The beam size at the sample is approximately 100 × 200 mm. The composition variation (or relative domain purity) over the length scales probed can be extracted by integrating scattering profiles to yield the total scattering intensity. The median domain spacing is calculated from $2\pi/q$, where q here corresponds to half the total scattering intensity. The purer the average domains are, the higher the total scattering intensity. Owing to a lack of absolute flux normalization, the absolute composition cannot be obtained only by R-SoXS.

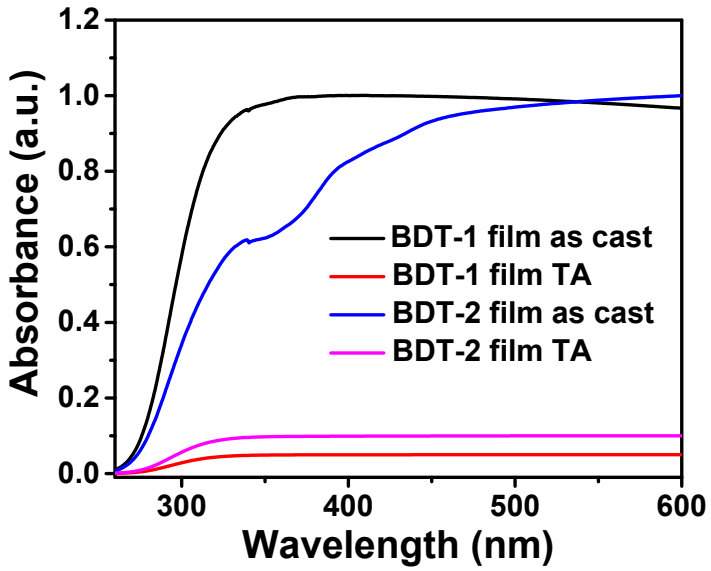

Fig. S1 The absorption profiles of pure BDT-1 and BDT-2 films with/without thermal annealing.

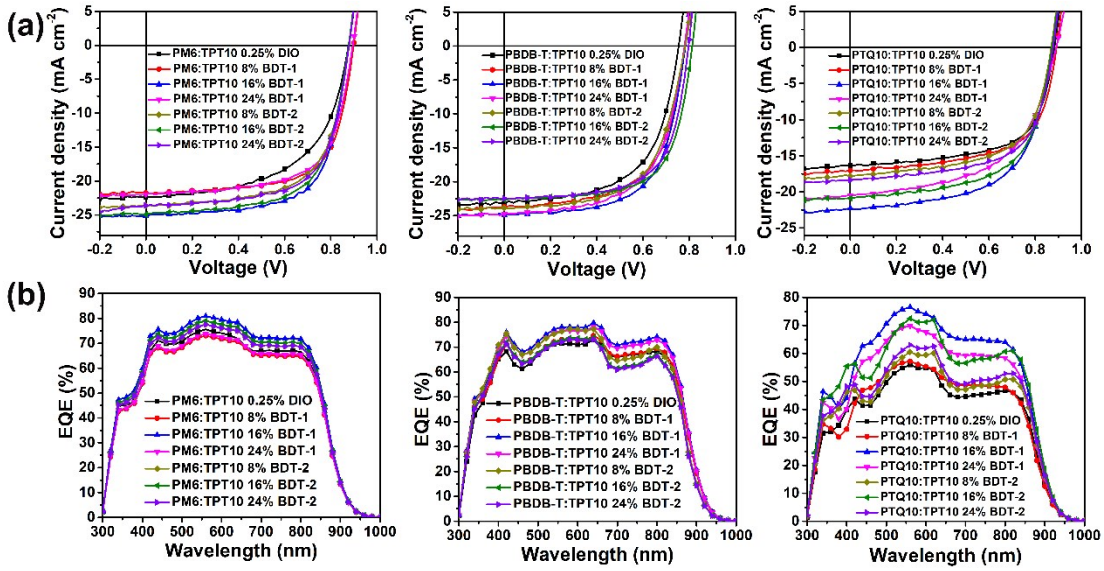

Fig. S2 (a) The *J*–*V* plots of the PM6:TPT10, PBDB-T:TPT10, and PTQ10:TPT10-based PSCs (1:1.2, w/w) with 0.25% DIO, different content of BDT-1 and BDT-2 additives after thermal annealing in the blend films under simulated AM 1.5G irradiation (100 mW cm^{-2}); (b) the corresponding EQE spectra of polymer solar cells.

Table S1 The photovoltaic parameters of the optimized PSCs (1:1.2, w/w) with 0.25%

DIO, different content of BDT-1 and BDT-2 additives after thermal annealing.

Active layer	Additives	TA	J_{SC} / calc. J_{SC}	V_{OC}	*FF* / %	PCE_{max} / %
PM6:TPT10	0.25% DIO	110 °C	22.40 / 21.23	0.877	68.6	13.55
	8% BDT-1	140 °C	23.10 / 21.95	0.899	71.0	14.74
	16 wt% BDT-1	140 °C	24.80 / 23.91	0.898	73.0	16.26
	24 wt% BDT-1	140 °C	22.90 / 21.75	0.895	72.0	14.77
	8% BDT-2	140 °C	23.60 / 22.44	0.878	68.7	14.21
	16 wt% BDT-2	140 °C	24.90 / 23.73	0.877	69.5	15.18
	24 wt% BDT-2	140 °C	23.60 / 22.46	0.879	68.3	14.17
PBDB-T:TPT10	0.25% DIO	110 °C	23.20 / 22.03	0.754	62.1	10.86
	8% BDT-1	140 °C	23.70 / 22.12	0.783	66.2	12.28
	16 wt% BDT-1	140 °C	24.90 / 23.73	0.783	68.8	13.41
	24 wt% BDT-1	140 °C	24.70 / 23.57	0.780	66.7	12.85
	8% BDT-2	140 °C	23.90 / 22.71	0.783	64.1	12.00
	16 wt% BDT-2	140 °C	22.70 / 21.53	0.813	68.3	12.60
	24 wt% BDT-2	140 °C	22.50 / 21.50	0.797	67.8	12.16
PTQ10:TPT10	0.25% DIO	70 °C	16.40 / 15.23	0.883	63.8	9.21
	8% BDT-1	140 °C	17.00 / 15.84	0.893	65.4	9.93
	16 wt% BDT-1	140 °C	22.30 / 21.15	0.890	66.2	13.14
	24 wt% BDT-1	140 °C	20.50 / 19.35	0.891	66.0	12.06
	8% BDT-2	140 °C	17.80 / 16.67	0.870	63.9	9.89
	16 wt% BDT-2	140 °C	20.90 / 19.73	0.873	66.8	12.37
	24 wt% BDT-2	140 °C	18.40 / 17.25	0.877	66.5	10.73

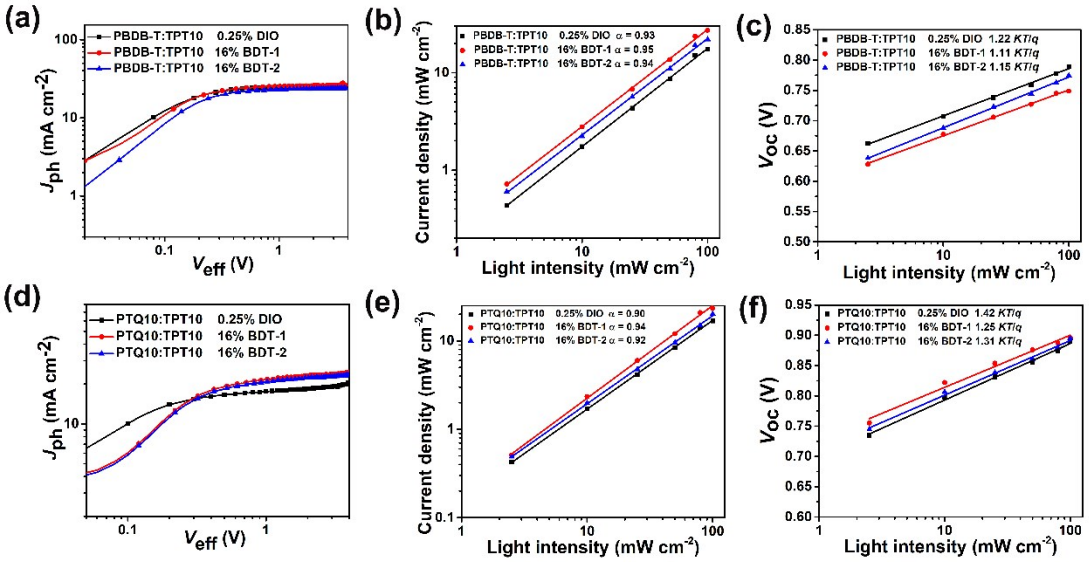

Fig. S3 J_{ph} - V_{eff} (a, d), J_{SC} - P (b, e), and V_{OC} - P (c, f) curves of PBDB-T:TPT10- and PTQ10:TPT10-based devices (1:1.2, w/w) with 0.25% DIO, 16 wt% BDT-1, and 16 wt% BDT-2 additives after thermal annealing. The solid lines indicate fitted curves in J_{SC} - P and V_{OC} - P plots.

Table S2 The exciton dissociation efficiency and charge collection efficiency of the PSCs (1:1.2, w/w) with 0.25% DIO, 16 wt% BDT-1, and 16 wt% BDT-2 additives after thermal annealing.

Blends	Additives	TA	J_{ph}	$J_{ph}^{\#}$	J_{sat}	η_{diss}	η_{coll}
PM6:TPT10	0.25% DIO	110 °C	22.41	20.83	24.51	91%	85%
	16 wt% BDT-1	140 °C	25.13	22.85	25.35	99%	90%
	16 wt% BDT-2	140 °C	24.89	22.34	25.39	98%	88%
PBDB-T:TPT10	0.25% DIO	110 °C	23.22	20.03	25.04	93%	80%
	16 wt% BDT-1	140 °C	24.88	22.08	25.67	97%	86%
	16 wt% BDT-2	140 °C	22.73	20.09	23.64	96%	85%
PTQ10:TPT10	0.25% DIO	70 °C	16.43	13.27	18.43	89%	72%
	16 wt% BDT-1	140 °C	22.35	18.93	23.37	95%	81%
	16 wt% BDT-2	140 °C	20.88	17.12	22.23	94%	77%

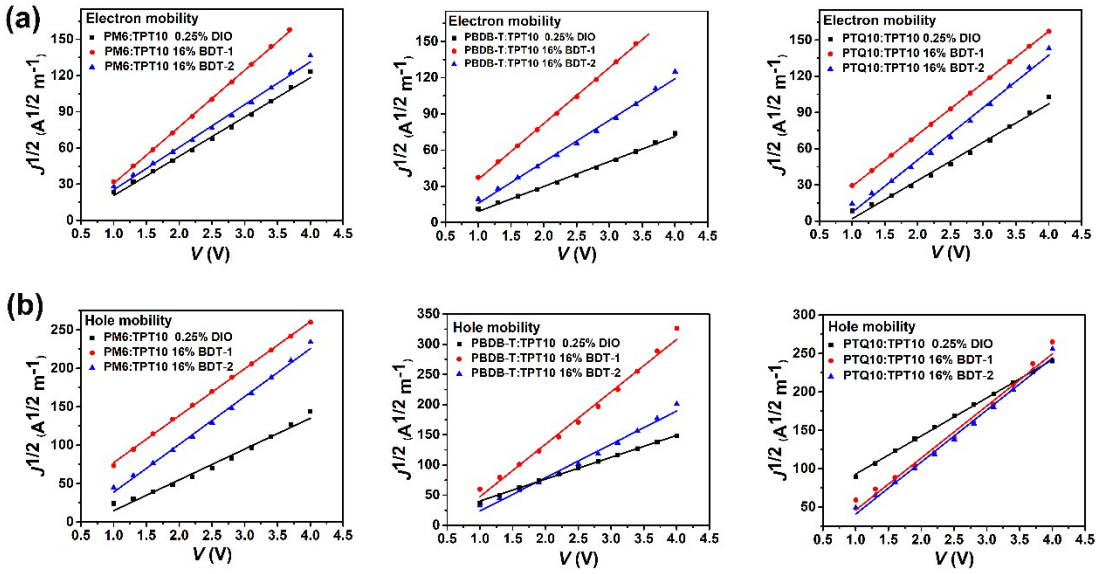

Fig. S4 *J–V* characteristics in dark for (a) electron-only and (b) hole-only of blends (1:1.2, w/w) with 0.25% DIO, 16 wt% BDT-1, and 16 wt% BDT-2 additives after thermal annealing.

Table S3 The hole and electron mobility values of the PM6:TPT10, PBDB-T:TPT10, and PTQ10:TPT10 blends (1:1.2, w/w) with 0.25% DIO, 16 wt% BDT-1, and 16 wt% BDT-2 additives afer thermal annealing measured by the SCLC method.

Active layer	Additives	TA	μ_e ß 10^{-4} (cm^2 V^{-1} s^{-1})	μ_h ß 10^{-4} (cm^2 V^{-1} s^{-1})	μ_e/μ_h
PM6:TPT10	0.25% DIO	110 °C	4.70±0.04	6.28±0.04	0.75
	16 wt% BDT-1	140 °C	6.75±0.03	7.16±0.05	0.95
	16 wt% BDT-2	140 °C	5.19±0.02	5.70±0.03	0.91
PBDB-T:TPT10	0.25% DIO	110 °C	2.41±0.04	3.50±0.05	0.69
	16 wt% BDT-1	140 °C	6.15±0.03	7.00±0.02	0.88
	16 wt% BDT-2	140 °C	5.81±0.03	6.80±0.07	0.85
PTQ10:TPT10	0.25% DIO	70 °C	1.45±0.04	2.50±0.06	0.57
	16 wt% BDT-1	140 °C	5.25±0.06	7.23±0.04	0.73
	16 wt% BDT-2	140 °C	5.10±0.04	7.29±0.05	0.70

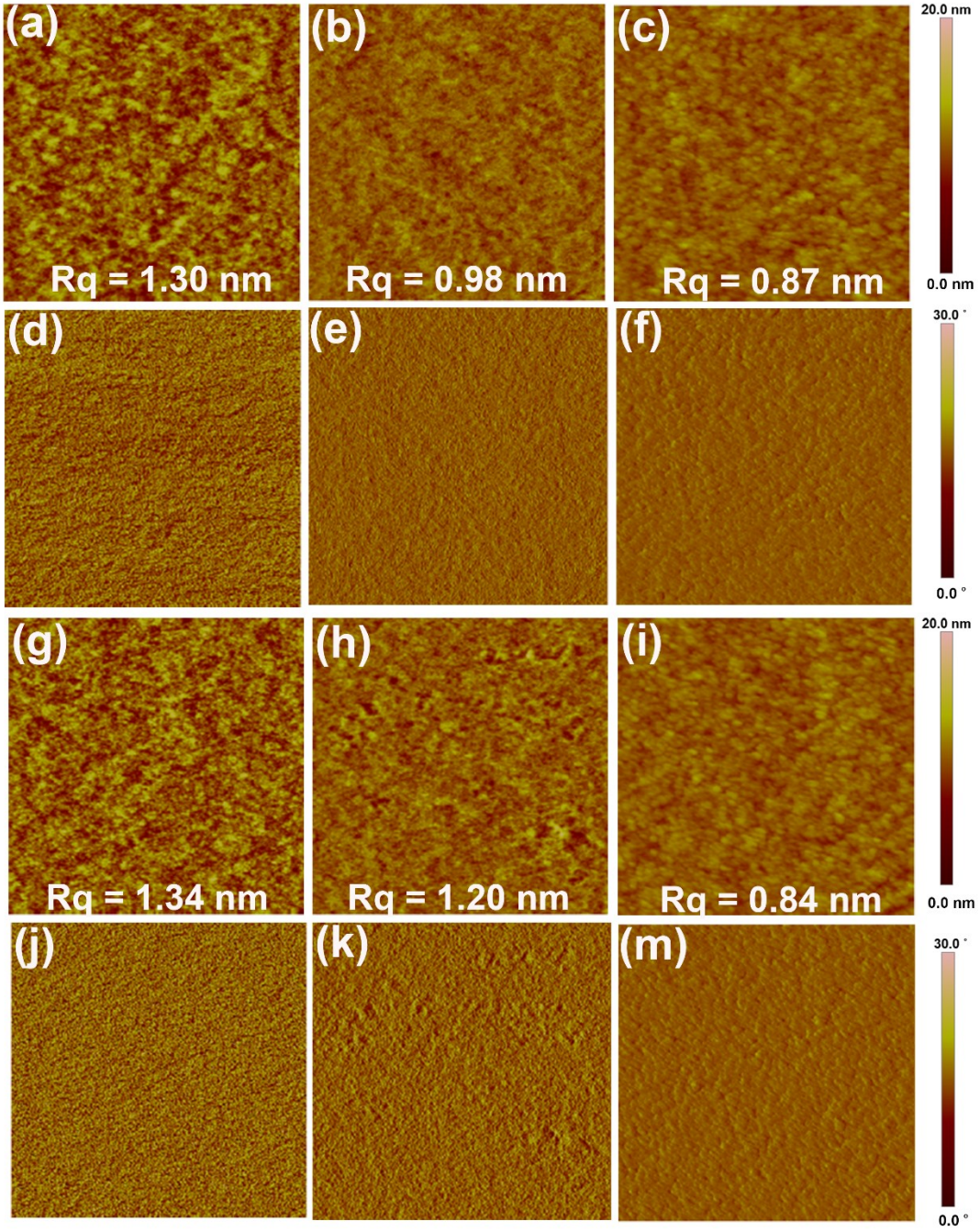

Fig. S5 AFM height (a, b, c, g, h, i) and phase (d, e, f, j, k, m) images of the PBDB-T:TPT10, and PTQ10:TPT10 blend films (1:1.2, w/w) with the additive treatment of 0.25% DIO (a, d, g, j), 16 wt% BDT-1 (b, e, h, k) and 16 wt% BDT-2 (c, f, i, m), respectively.

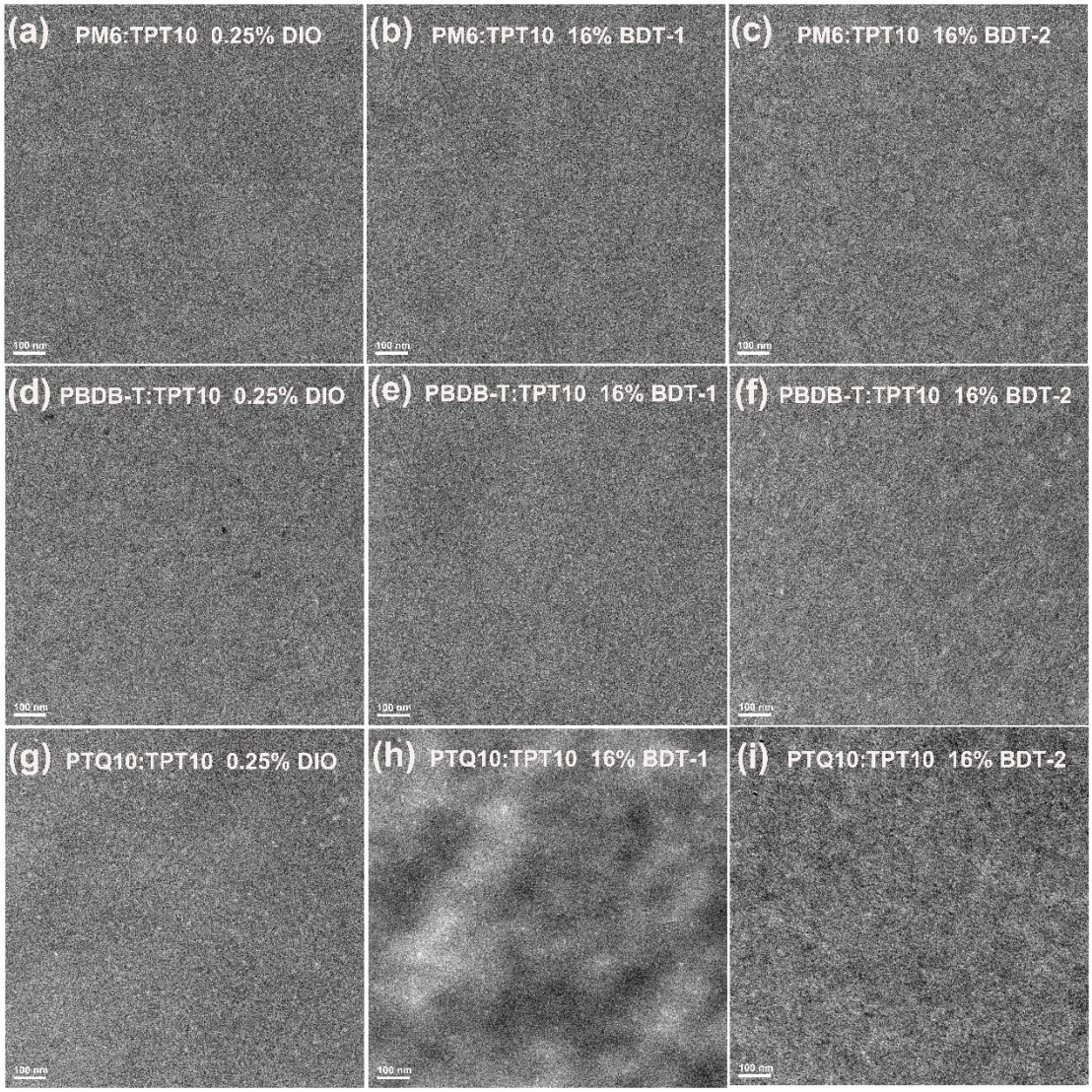

Fig. S6 TEM images of PM6:TPT10, PBDB-T:TPT10 and PTQ10:TPT10 (1:1.2, w/w) blends with 0.25% DIO (a, d, g), 16 wt% BDT-1 (b, e, h), and 16 wt% BDT-2 (c, f, i) additives after thermal annealing.

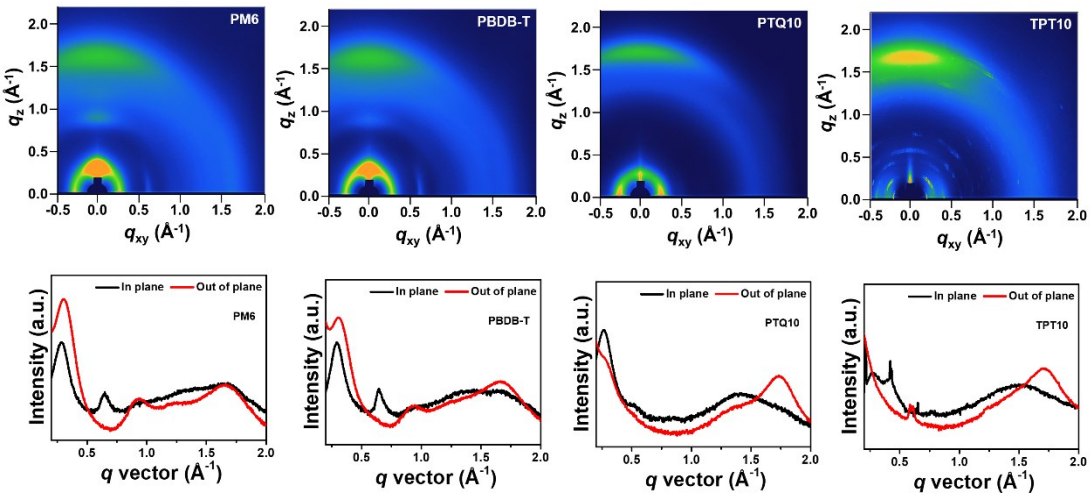

Fig. S7 2D GIXS patterns of pure PM6, PBDB-T, PTQ10, and TPT10 films with 0.25% DIO, 16 wt% BDT-1 and 16 wt% BDT-2 additives after thermal annealing, and the corresponding GIXS intensity profiles along the in-plane (black line) and out-of-plane (red line) directions.

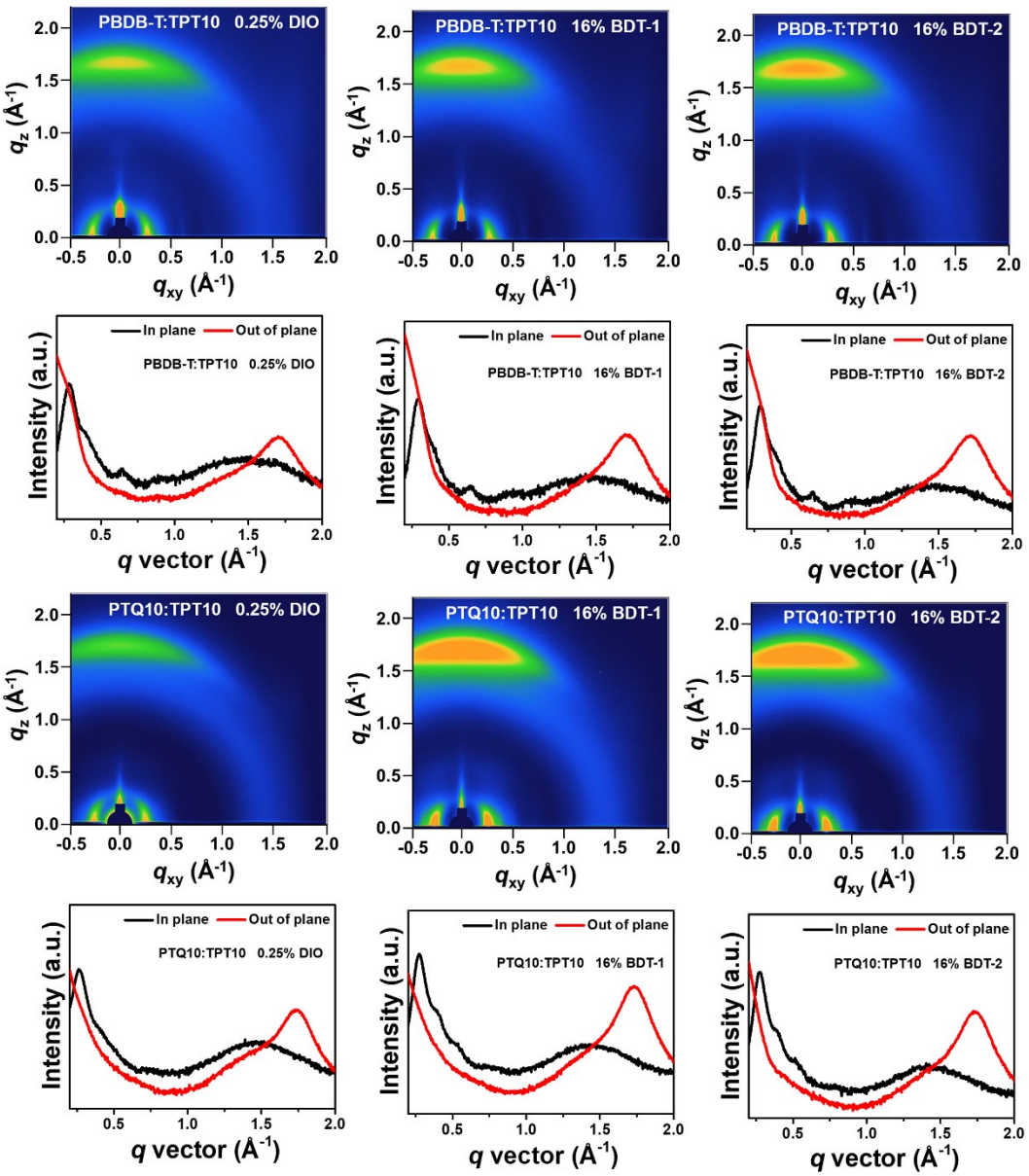

Fig. S8 2D GIXS patterns of PBDB-T:TPT10 and PTQ10:TPT10 (1:1.2, w/w) blends with 0.25% DIO, 16 wt% BDT-1, and 16 wt% BDT-2 additives after thermal annealing, and the corresponding GIXS intensity profiles along the in-plane (black line) and out-of-plane (red line) directions.

Table S4 Relative data of pure PM6, PBDB-T, and PTQ10 films and PM6:TPT10, PBDB-T:TPT10, and PTQ10:TPT10 (1:1.2, w/w) blend films with 0.25% DIO, 16 wt% BDT-1, and 16 wt% BDT-2 additives after thermal annealing obtained from GIXS measurement.

Films	Out-of-Plane						In-Plane					
	π-π stacking cell axis (010)			lamellar stacking cell axis (100)			π-π stacking cell axis (010)			lamellar stacking cell axis (100)		
	q ($Å^{-1}$)	d-spacing (Å)	Coherence length (Å)	q ($Å^{-1}$)	d-spacing (Å)	Coherence length (Å)	q ($Å^{-1}$)	d-spacing (Å)	Coherence length (Å)	q ($Å^{-1}$)	d-spacing (Å)	Coherence length (Å)
PM6	1.66	3.78	18.69	0.30	21.00	46.56		N/A		0.28	22.16	56.75
PBDB-T	1.68	3.75	22.36	0.30	21.22	39.55		N/A		0.29	21.40	64.38
PTQ10	1.72	3.65	26.02		N/A			N/A		0.26	23.82	62.32
TPT10	1.69	3.72	20.26		N/A			N/A		0.28	22.52	75.22
PM6:TPT10 (0.25% DIO)	1.70	3.70	23.51		N/A			N/A		0.29	21.87	70.00
PM6:TPT10 (16 wt% BDT-1)	1.70	3.70	24.08		N/A			N/A		0.29	21.51	82.83
PM6:TPT10 (16 wt% BDT-2)	1.70	3.69	24.25		N/A			N/A		0.29	21.59	82.54
PBDB-T:TPT10 (0.25% DIO)	1.69	3.72	22.81		N/A			N/A		0.28	22.16	71.97
PBDB-T:TPT10 (16 wt% BDT-1)	1.70	3.70	23.62		N/A			N/A		0.29	21.67	87.55
PBDB-T:TPT10 (16 wt% BDT-2)	1.70	3.69	24.24		N/A			N/A		0.29	21.63	97.11
PTQ10:TPT10 (0.25% DIO)	1.73	3.64	25.62		N/A			N/A		0.27	23.69	81.95
PTQ10:TPT10 (16 wt% BDT-1)	1.726	3.65	28.12		N/A			N/A		0.27	23.03	94.43
PTQ10:TPT10 (16 wt% BDT-2)	1.728	3.64	27.89		N/A			N/A		0.27	22.99	96.40

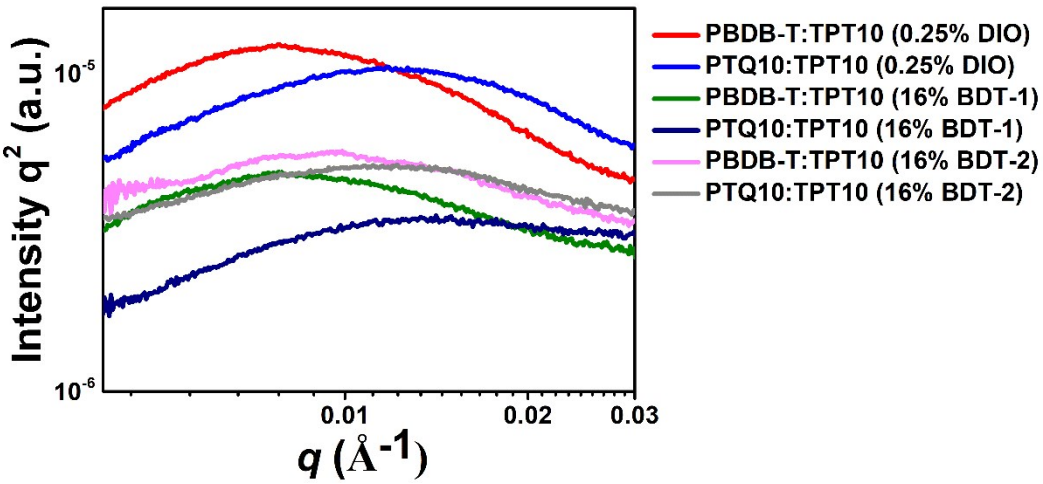

Fig. S9 R-SoXS profiles for PBDB-T:TPT10 and PTQ10:TPT10 (1:1.2, w/w) blends with 0.25% DIO, 16 wt% BDT-1, and 16 wt% BDT-2 additives after thermal annealing.

Table S5 Relative data of PM6:TPT10, PBDB-T:TPT10 and PTQ10:TPT10 (1:1.2, w/w) blend films with 0.25% DIO, 16 wt% BDT-1, and 16 wt% BDT-2 additives after thermal annealing obtained from RSoXS measurement.

Blends	Additives	q_{peak} (Å^{-1})	Domain spacing (nm)	Relative domain purity
PM6:TPT10	0.25% DIO	0.099	63.5	1
	16 wt% BDT-1	0.097	64.7	0.82
	16 wt% BDT-2	0.124	50.8	0.70
PBDB-T:TPT10	0.25% DIO	0.080	78.3	0.90
	16 wt% BDT-1	0.077	81.4	0.66
	16 wt% BDT-2	0.095	66.0	0.73
PTQ10:TPT10	0.25% DIO	0.121	51.8	0.93
	16 wt% BDT-1	0.137	49.6	0.68
	16 wt% BDT-2	0.115	54.8	0.74

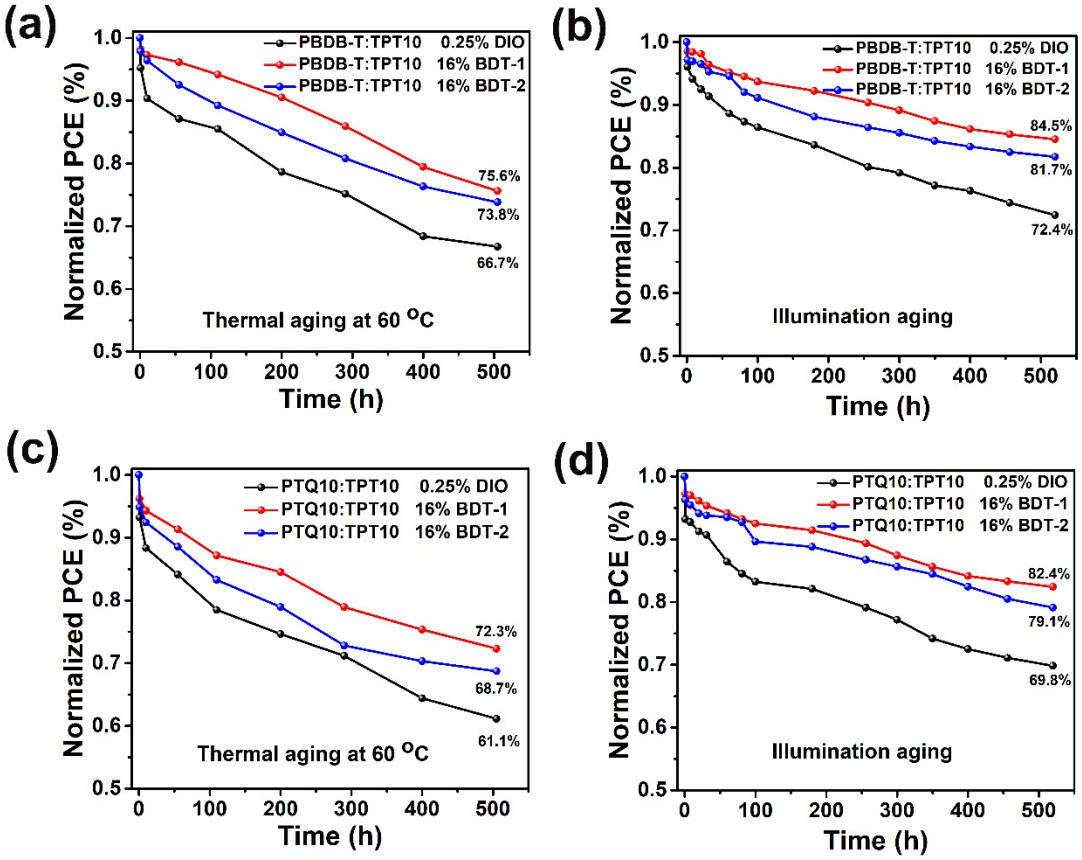

Fig. S10 Normalized PCEs of the PBDB-T:TPT10 and PTQ10:TPT10 (1:1.2, w/w) based device with 0.25% DIO, 16 wt% BDT-1, and 16 wt% BDT-2 additives after thermal annealing at the 60 °C thermal aging time (a) and illumination aging time (under continuous 1 sun illumination) (b) in a nitrogen-filled glovebox, respectively.